Available online at www.sciencedirect.com
ScienceDirect
Journal of the European Ceramic Society 29 (2009) 23–30
www.elsevier.com/locate/jeurceramsoc

Incorporation of wastes from granite rock cutting and polishing industries to produce roof tiles

P. Torres, H.R. Fernandes, S. Olhero, J.M.F. Ferreira *

Department of Ceramic and Glass Engineering, University of Aveiro, 3810-193 Aveiro, Portugal

Received 5 January 2008; received in revised form 30 April 2008; accepted 24 May 2008
Available online 17 July 2008

Abstract

The present work aimed at studying the incorporation of wastes from natural rock cutting and polishing to produce roof tiles. The sintered products incorporating the sludge were targeted to have similar or even enhanced properties in comparison to those made of a standard reference paste industrially used to fabricate concurrent products available in the market. Firstly, the raw materials, including the sludge, were characterised by particle size distribution, density, X-ray diffraction (XRD), thermal properties and loss on ignition. Different formulations were prepared to evaluate the effects of each component on plasticity of pastes, drying and firing processes, and on the final properties of the tiles. Finally, the most promising formulations were selected and characterised for sintered density, water absorption, and flexural bending strength. The results obtained made it possible to conclude about the possibility of producing roof tiles incorporating 10% of granite wastes having excellent properties (water absorption <6%, lower pyroplastic deformation index, and bending strength values of about 14 MPa and 38 MPa for the green and sintered products, respectively). Therefore, the sludge derived from the granite cutting and polishing industries can be classified as a by-product suitable to replace natural non-plastic raw material in traditional ceramic formulations. This will contribute to preserve non-renewable natural resources, while it allows minimization of the negative environmental impact due to its disposal.

Keywords: Recycling; Sludge; Granite; Roof tiles; Waste materials

1. Introduction

The technological development and the increasing rate at which raw materials are continuously transformed into industrial products result in environmental aggressions and waste generation, which affect public health. Besides creating negative environmental impacts, the accumulation of industrial residues also opposes sustainable development. In the last decades the environmental considerations appeared as a main concern for most of the developed countries and efforts to reuse residues have been undertaken. At present, the business conscience of recycling stimulates both small and big enterprises to look for alternative solutions aiming at recycling and adding commercial value to the final products taking into consideration the environmental legislation, especially within the Member States of European Union (EU).[1] The waste management must be done in accordance with certain standards and in cases of damage to the environment the operator is liable.[2]

The industry of the ornamental granite is included in the natural stone industry sector, more specifically in the sub-sector of the ornamental rocks comprising the extraction and processing of rocks for ornamental applications. This economical activity represents an important sector in the worldwide economy.[3] For the Portuguese economy, the importance of this industrial sector is mostly due to its exportation component. In 2004, Portugal exported 334,751 tons of granite and similar rocks (about 39 million €).[3] A less known aspect of the exploration of the ornamental rocks is the great volume of produced residues, specifically, solids (generated during the extraction) and sludges (produced during the transformation process). Deposition in surface landfills is the most current destiny of these residues. These materials can be deposited as dry particles with large particle size range or as fine particles in aqueous environment, generally deposited by sedimentation.[4] It is also common to deposit filter-pressed sludges in surface landfill. Although not considered dangerous,[5] incorrectly planned deposition of these

* Corresponding author.
E-mail address: jmf@ua.pt (J.M.F. Ferreira).

0955-2219/$ – see front matter © 2008 Elsevier Ltd. All rights reserved.
doi:10.1016/j.jeurceramsoc.2008.05.045

residues can cause accidents and environmental impact like, for example, the increase of the turbidity of the courses of water, a fact that provokes the reduction of light penetration leading to a reduction of photosynthesis, reduction of the productivity of lively organisms, reduction of the nutritious ones, alteration of the food chain and loss of aesthetic value.[6] The dried mud is easily dragged by the wind and becomes harmful to humans and animals through its inspiration or to plants when deposited on their leaves.[7–10] The sludges generated during the processing of stone have no specific practical applications and have been managed as waste. It has been estimated that the sawdust, cutting and polishing processes produce about 0.1 m^3/ton of processed rock, 0.08 m^3/ton in the operation of sawdust and 0.02 m^3/ton in the operations of cutting and polishing. In Portugal, in 1998 about 27,133 ton of this waste was generated.[4] However, given the current rate of production, this figure should be much higher after about a decade. Since the transport and deposition of waste in landfills involve significant costs, its incorporation in other industrial processes could lead to the reduction of costs and open new business opportunities, while reducing the volume of extraction of raw materials, preserving limited natural resources. Thus, recycling of waste emerges as an opportunity to transform a considerable expense into profit or, at least, in the reduction of the deposition costs. Besides the civil construction, the ceramics industry is one of the sectors that consumes large amount of natural resources and seems to be one of the most indicated sectors to absorb this type of waste. Some previous studies showed that granite sludge (GS) has a high potential as raw material in the ceramic industrial sector.[11–17]

In the present work, the incorporation of granite wastes in red clay roof tiles formulations was studied aiming at improving the technical and aesthetical properties of the final products. The main goal was to produce roof tiles that exhibit lower water absorption values (<6%) when compared to a reference commercial formulation (8–9%) without increasing the sintering temperature, and to reduce the pyroplastic deformation of the tiles during firing and the overall production costs.

2. Materials and experimental procedure

GS was supplied by Incoveca (Viseu, Portugal), whose main activity is related to ornamental rock cutting and polishing. The as-received GS, containing about 25% moisture, was dispersed in water, passed through a 500 μm sieve, dried at 110 °C and disaggregated using a hammer-mill. Taking into account previous studies concerning the incorporation of granite residues in red clay (RC) ceramic formulations,[13–15] several batches incorporating up to 30 wt.% of GS were prepared. A commercial reference paste (T) supplied by a roof tiles producer, Cerâmica Sotelha S.A. (Aveiro, Portugal) was used for comparison purposes. This paste comprises yellow clay (YC) and red plastic RC in undisclosed proportions. In the new formulations (Table 1), YC was not used because it has now revealed to be compositional inconstant and was replaced by alternative raw materials such as red clay (RC2) and a white sludge (WS) resultant from a silica sand-washing process. RC1 was kept in the tested formulations because it is the main clay component in paste T and its extraction belongs to Cerâmica Sotelha S.A. The as-received raw materials were dried at 70 °C and disaggregated using a hammer-mill.

Table 1
The proportions of the blends in the tested formulations (in wt.%)

Formulation	Clay RC1	Clay RC2	Sludge WS	Sludge GS
T	Reference paste			
1	40	40	20	–
2	40	40	10	10
3	40	30	30	–
4	40	30	20	10
5	40	30	–	30
6	40	20	40	–

The batches were prepared by mixing raw materials with water under mechanical stirring. The homogenized mixtures were then dried at 110 °C, and disagglomerated by gently grinding in a porcelain mortar. Preliminary tests were performed by preparing pellets (Ø 20 mm, weight 2 g) by cold uniaxial pressing at 47 MPa and sintering in a laboratory furnace at 1000 °C for 1 h in air (heating–cooling rate 5 °C/min). Density of green and sintered samples was determined using the Archimedes method by immersing in Hg. Water absorption was measured according to the ISO-standard 10545-3, i.e. weight gain of dried pellets after immersion into boiling water for 2 h, cooling for 3 h and sweeping of the surface with a wet towel.[18] The characterization of these preliminary testing samples made it possible to select the formulations showing lower water absorption values.

Batches weighing 6 kg were prepared as follows: the dried raw materials were weighted, mixed and moistured with 14–18 wt.% water, and extruded in a laboratorial vacuum extruder (NR Burton on Trent, Rawdon Ltd., Moira, UK) to produce cylindrical testing samples (Ø 10 mm, length ∼130 mm). These samples were marked with 100 mm distance scratches to measure the shrinkage after drying and after sintering. The extrusion ability (i.e. plasticity) of the resulting pastes was evaluated with the Atterberg method. The paste moisture was measured using a humidity balance (AE Adam Equipment Co., Ltd., model AMB310, UK). Samples were sintered in a laboratorial furnace (950 °C, 1000 °C, and 1050 °C; heating/cooling rate: 5 °C/min; and dwell: 1 h) and in an industrial tunnel kiln at Cerâmica Sotelha S.A. (909 °C for 4.5 h at the maximum temperature, with total cycle of 30 h and 959 °C for 4 h at the maximum temperature with total cycle of 32 h). The sintering temperature was controlled using the pyrometers and process temperature control rings (Ferro Electronics Materials B.V., PTCR—LTH and PTCR—ETH, Netherlands) placed closed to the samples.

Besides the above-mentioned water absorption and density measurements of green and sintered samples, several other characterization tests were conducted during the entire process, including the following techniques. Plasticity limits and the plasticity index were determined by the method of Atterberg. The true density of the dried powders and of the samples was determined by the helium picnometer (Multipycnometer Quantumchrome, USA). Particle size distribution was measured using a light scattering instrument (Coulter LS 230,

UK, Fraunhofer optical model) and complemented by measuring the weight percent of particles retained on the 125 μm sieve. Chemical compositions of the clays and of the sludges were determined through X-ray fluorescence analysis (X-ray spectrometer, PW1400, Philips, Netherlands). The mineralogical characterization and the identification of the crystalline phases were performed through an X-ray diffractometer (XRD, Rigaku GeigerflexD/Mac, C Series, Cu Ka radiation, Japan), complemented with differential (DTA) and gravimetrical (TG) thermal analyses (Setaram Labsys TG-DTA/DSC, France, heating rate 5°/min, 1 atm flowing N_2) and dilatometer thermal analysis (Bahr thermo analyse DIL 801 L, Germany, heating rate 10 °C/min). Pyroplastic deformation index also was determined at different temperatures for the most promising formulations. The flexural strength of the samples was determined in three-point bending tests (Shimadzu Autograph, Japan) with a constant crosshead speed of 0.5 mm/min. The presenting results are the average of at least 12 tested samples. Retraction and weight loss measurements during drying and sintering were also carried out.

3. Results and discussion

3.1. Characterization of raw materials

The data of chemical composition and loss on ignition of the raw materials are presented in Table 2. It can be observed that in all of them, SiO_2 is the predominant oxide, followed by Al_2O_3. GS presents a significant amount of iron. Although it has been expressed in terms of Fe_2O_3 (10.63 wt.%), some iron consists of fine, abrasive shoot particles used in the granite cutting operation. This procedure uses a suspension comprising calcium hydroxide $Ca(OH)_2$, stone powder, and hard iron shoot. The presence of calcium hydroxide can explain the occurrence of CaO in GS, although the presence of marble residues in the sludge can also explain the occurrence of this oxide, because the supplier company also transforms marble stones. Iron oxide is an auxiliary fluxing agent and is responsible for the reddish colour of sintered products. It is a desirable constituent for clay-based materials of red colour after sintering.[19] GS also exhibited a high amount of fluxing oxides ($K_2O + Na_2O$) and auxiliary fluxing oxides ($Fe_2O_3 + CaO + MgO$) that are expected to form a more abundant glassy phase or its formation at lower temperatures.

Table 2
Chemical composition of the raw materials (wt.%)

Oxides	RC1	RC2	WS	GS
SiO_2	60.00	67.41	54.03	62.70
Al_2O_3	20.00	16.77	28.88	12.75
Fe_2O_3	5.90	4.60	1.97	10.63
CaO	0.70	0.16	0.07	3.96
MgO	1.90	0.43	0.28	0.80
Na_2O	<0.50	<0.20	0.23	3.34
K_2O	3.00	1.32	3.20	4.34
TiO_2	0.80	0.93	0.38	0.24
MnO	<0.30	<0.02	0.02	0.10
P_2O_5	<0.5	0.06	0.08	0.26
L.O.I.	6.70	8.00	10.63	0.70

Table 3
Mineral phases identified in the raw materials

Raw materials	Total sample	Sample <2 μm
RC1	Quartz, kaolinite, illite, montmorilonite	Quartz, kaolinite, illite, montmorilonite, microcline
RC2	Quartz, kaolinite, calcite	Quartz, kaolinite, illite, montmorilonite, microcline
WS	Quartz, kaolinite, illite, microcline	Quartz, kaolinite, illite, microcline
GS	Quartz, kaolinite microcline, albite e illite, calcite	–

Table 3 shows the mineral phases identified in the X-ray diffraction (XRD) spectrograms of raw materials. The identification of clay minerals was complemented by the specific diffraction tests using material with preferential orientation in order to highlight the reflections corresponding to basal plans. According to Table 3, all raw materials contain quartz [SiO_2], kaolinite [$Al_2Si_2O_5(OH)_4$], illite, [$(K,H_3O)Al_2Si_3AlO_{10}(OH)_2$] (RC2 presented illite peaks only in sample <2 μm), and microcline [$KALSi_3O_8$] (the red clays showed microcline peaks only in sample <2 μm), which suggests that feldspar consists of finer particles than quartz, which shows high relative intensity peaks that tend to mask the presence of feldspar. GS and RC2 are richer in quartz while WS is richer in kaolinite. These results were also supported by thermal analysis (not presented), confirming that RC1 and RC2 contain low amounts of montmorilonite. Calcite was detected in RC2 and GS. This last sludge also contains albite [$NaAlSi_3O_8$]. All minerals present in GS are common to ceramic raw materials.

Table 4 presents some physical properties of raw materials. The density of GS is slightly higher in comparison to the other raw materials and is also higher than typical density value for granite (2.55–2.75 g/cm^3). This is due to the presence of iron shoot particles in GS (10.63 wt.% Fe_2O_3, Table 2). The volume percent values corresponding to particles with sizes <2 μm suggest that RC1 with the highest percentage (50%) is the most plastic raw material. Although WS showed the highest loss on ignition (Table 2), its volume percent of particle lower than 2 μm is not so high, confirming that this raw material is rich in clay minerals from kaolinite group (Table 3), comprising high amount of constitutional water (13–14%). This fact was supported by thermal analysis (not presented). Considering the particles size data gathered by light scattering, it is apparent that

Table 4
Physical properties of the raw materials

Raw materials	RC1	RC2	WS	GS
Density (g cm^{-3})	2.39	2.69	2.50	2.77
Mean particle size (μm)	2.7	5.6	11.0	16.5
Maximum particle size (μm)	12	25	53	100
Particles <2 μm (vol.%)	50.0	36.6	18.9	17.2
Particles 2–60 μm (vol.%)	50.0	63.4	81.1	78.8
Particles >60 μm (vol.%)	–	–	–	4.0

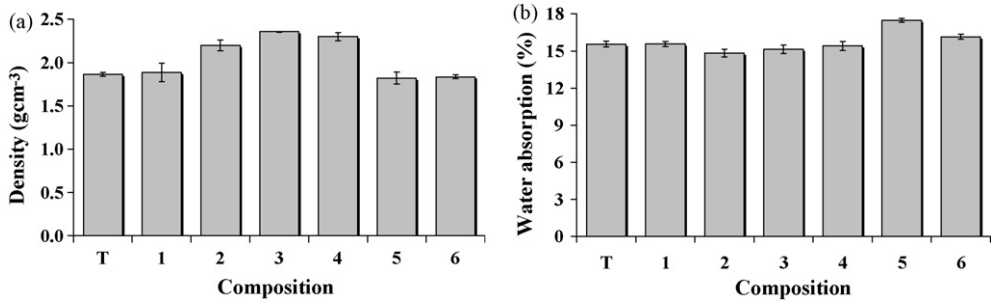

Fig. 1. Variation of green density (a), and of water absorption (b), after being sintered in an electrical furnace at 1000 °C for 1 h for the different compositions consolidated by dry pressing.

only GS presents a small (4%) volume fraction of particles with sizes >60 μm, i.e. the sand fraction.

3.2. Selection of compositions from the results of dry-pressed samples

For a given batch formulation, the green density is closely related to the particle size distribution, the shape of particles, and mineralogical composition of ceramic paste, being an important parameter in the case of roof tiles that are sintered at low relatively temperature.[20] A good packing degree and the close contact between the constituent particles enhance the reaction rates upon sintering, leading to higher shrinkage values and final products with better mechanical resistance.

Fig. 1(a) shows the dependence of apparent green density of dry-pressed samples on the tested compositions, while Fig. 1(b) presents the data of water absorption after firing the samples at 1000 °C for 1 h. Water absorption can be regarded as an indirect method to predict the technological properties of the final products since the measured values are closely related to the microstructure of the sintered sample. The comparison of Fig. 1(a) and (b) reveals that high green densities generally correspond to lower water absorption values. These results confirm the importance of a good particle packing during the ceramic body conformation process, which is only dependent on the batch composition since the same processing and consolidation conditions were used for all the samples. In the formulations comprising 40% RC1 and 30% RC2 (compositions 3, 4, and 5), increasing the amount of GS (in substitution of WS) resulted in lower apparent densities of the green samples and higher water absorption values of the sintered ones. However, the same trend is not verified for compositions with 40% RC1 and 40% RC2 (compositions 1 and 2) in which the replacement of 10% of WS by the same amount of GS led to an increase in green density and to a decrease of water absorption after sintering.

Comparing the values obtained for compositions 2 and 3 comprising equal contents of RC1, it can be observed that the increase from 10 to 30% of WS at the expenses of 10% reduction of each RC2 and GS resulted in an increase of green density and in a slight increase in values of water absorption, contrary to the previously observed trend. This can be understood considering that WS comprises a higher amount of caulinite, making it more refractory. Based on these results, formulations 2 and 3 (Table 1) were selected to continue the work because of their lower values of water absorption. These two formulations, together with the reference paste were prepared at a larger scale and extruded to produce cylindrical testing samples for the evaluation of the technological properties and to study the extrusion ability, as discussed in the next section.

3.3. Technological characterization of the selected formulations

The particle size distributions of selected pastes as measured by light scattering are represented in Fig. 2(a). Reference paste T presents a Gaussian distribution with mean size of 7.3 μm. The mean particle sizes of compositions 2 and 3 are equal to 7.8 μm and 6.7 μm, respectively. Composition 2 contains about 32 vol.% of particles smaller than 2 μm while the fine fractions in compositions 3 and T are about 29 vol.% and 24 vol.%, respectively. This suggests that compositions 2 and 3 are more plastic than T, since particles smaller than 2 μm correspond mainly to

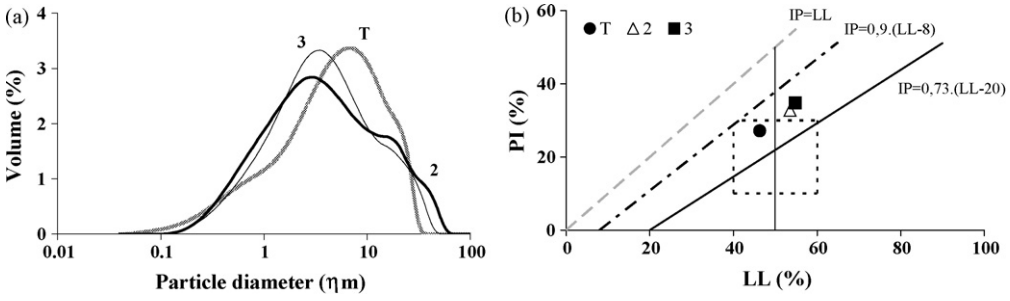

Fig. 2. Particle size distribution (a) and Casagrande's diagram (b) for selected compositions (2 and 3) and reference paste (T). The pointed square represents the optimal plasticity for extrusion.

clay minerals. The maximum particle sizes determined by this technique for the different compositions were 40 μm (T), 53 μm (3), and a bit less than 70 μm (2). However, it should be stated that the coarser particles present in the different formulations could not be easily detected by light scattering. The main reason is the rapid sedimentation of the coarser particles to the bottom of the beaker from the much diluted suspensions used. To cope with this limitation, the formulations were passed through a 125 μm sieve and the values of weight percent particles retained in this sieve were determined as 7.43 wt.% (T), 1.01 wt.% (2) and 0.90 wt.% (3), conforming that the reference paste contains a significant fraction of coarse particles.

The plasticity tests performed on selected pastes are represented in Casagrande's diagram showed in Fig. 2(b). Pastes 2 and 3 have higher plasticity index (32.7 and 34.8%, respectively) than reference paste T (27.1%). This can be explained by the particle size distribution (Fig. 2(a)), particularly, by the portion of particles smaller than 2 μm, present in the pastes. The nature of the predominant clay minerals is also an important factor. Paste 3 is only based on clayey components, thus explaining its highest plasticity index. Although in the Casagrande's diagram, pastes 2 and 3 are located outside the considered optimal area for good extrudability, which corresponds to the pointed square in Fig. 2(b),[21] the extruded samples did not exhibit any problem during conformation and drying processes.

Fig. 3 presents and compares the firing behaviour, and the properties of selected compositions with those of the commercially formulated T after sintering at several temperatures in an electrical laboratory furnace and in an industrial kiln. As a matter of fact, the sintering cycle (temperature, time, heating, and cooling rate) is one of the most important factors in the densification process of a ceramic body. According to Jouenne,[22] the expansion of a raw material or raw pulp corresponds roughly to the algebraic sum of dilatations of the mineral constituents, taking into account their volume proportions in the ceramic body (including porosity). Under this perspective, it is possible to analyse the dilatometric curves using the typical curves of individual minerals. The dilatometric behaviour of the tested pastes upon firing up to 1100 °C is illustrated in Fig. 3(a). Compositions 2 and 3 displayed similar dimensional variations upon firing. All compositions revealed a small initial retraction, probably due to the release of adsorbed water, followed by a slow gradual thermal expansion, higher in T, apparently due to a higher amount of quartz in this composition. This is supported by (i) the strong expansion associated with the transformation of quartz-α into quartz-β, which occurs typically in the range 573–575 °C, being more evident for paste T and masking the effects of trans-

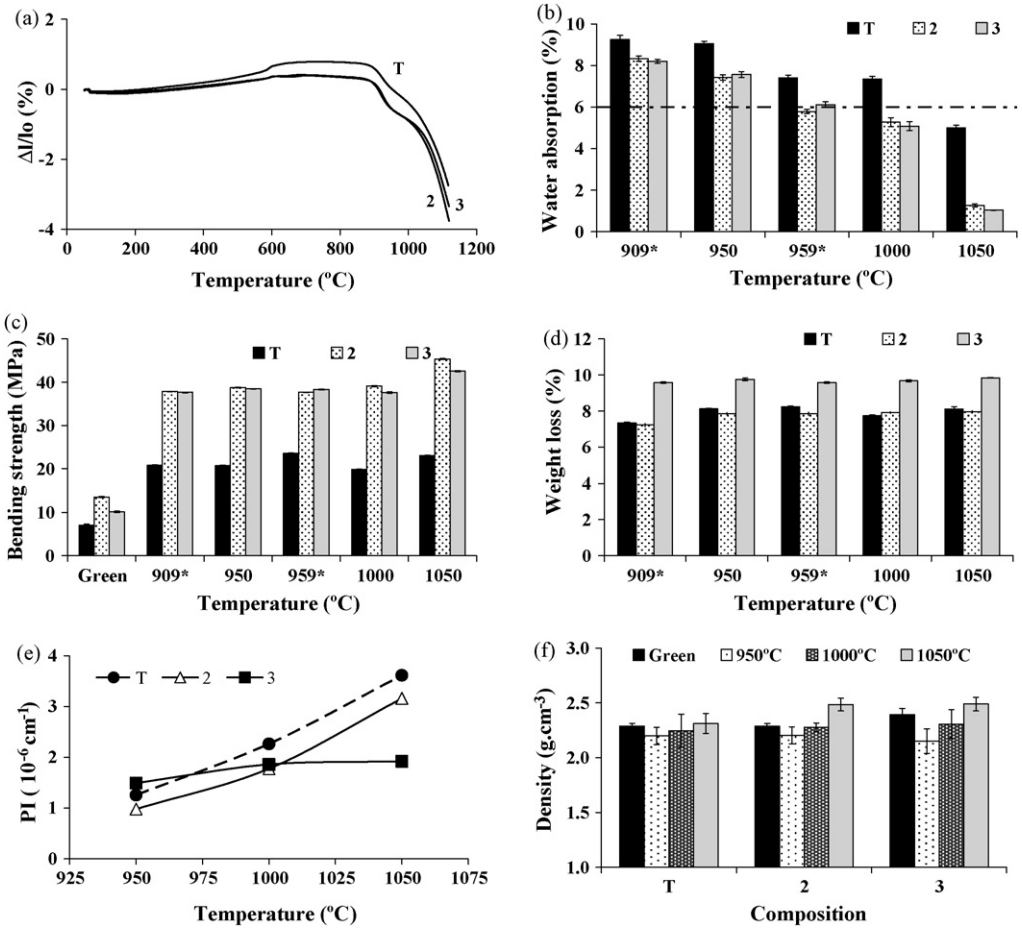

Fig. 3. Properties of extruded samples before and after being sintered at several temperatures both in laboratory and industrial furnaces: (a) dilatometric behaviour of pastes up to about 1100 °C; (b) water absorption; (c) bending strength; (d) weight loss during sintering; (e) pyroplastic index and (f) apparent density after sintering.

formation of kaolinite into meta-kaolin; (ii) the higher wt.% of particles retained in the 125 μm sieve. In the range 610–870 °C, the dimensional variations are negligible corresponding to typical behaviour of compositions comprising quartz, kaolinite, and illite.[23] Above 870 °C it is possible to observe retractions caused by the presence of kaolinite and illite, leading to sample dimensions lower than the green ones at about 900 °C, 910 °C and 950 °C for pastes 2, 3 and T, respectively. Between about 950 °C and 1030 °C the retraction rate decreases for all pastes, being more evident in the cases of pastes 2 and 3. This is probably due to the higher amounts of kaolinite present in these pastes and to the transformation of meta-kaolin into spinel with the ejection of amorphous silica and the formation of primary mullite crystals that begin to develop in the clay relicts at 1000 °C or above.[24] The sintering phenomena are then accelerated at temperatures of about 1030 °C, being translated by a faster shrinkage rate.

Fig. 3(b) displays the variation of water absorption values with sintering temperature for the tested compositions. As expected, these values are lower than those obtained in the preliminary tests from dry-pressed pellets, since the homogeneity is higher in the case of vacuum extruded samples. On the other hand, the target value of <6% for water absorption has been achieved for the new formulations sintered at temperatures ≥960 °C, contrarily to what has been observed for the reference paste.

The water absorption values, related with open porosity, decrease with increasing sintering temperature for all compositions. Pastes 2 and 3 presented similar behaviour and lower water absorption values than T. Above 1000 °C, the more accented reduction of water absorption values for pastes 2 and 3 suggests a better densification probably due to the formation of a more abundant glassy phase or the absence in these compositions of the coarse and low plasticity yellow clay used in the reference paste. Accordingly, pastes 2 and 3 exhibit significantly higher bending strength values than T, both in green state and after sintering as illustrated in Fig. 3(c). The highest bending strength values for green samples of paste 2 might be due to the beneficial effects of GS on the drying step.

The weight loss experienced by the samples upon sintering is illustrated in Fig. 3(d). There are no significant differences in weight loss between the reference paste and composition 2. However, composition 3 presents weight loss values that are about 1–1.2% higher, probably because it is richer in clay minerals. This is not surprising since the weight loss is mainly due to the elimination of constitution water of clay minerals that occurs at lower temperatures.[23,24]

The values of pyroplastic index, PI, are plotted in Fig. 3(e). PI reflects the tendency of the pastes to deform upon firing. It can be seen that at 950 °C all the tested compositions show similar and relatively low PI values. However, the differences start to reveal more clearly at temperatures ≥1000 °C with the reference paste exhibiting higher values. These results show that the reference paste is the most susceptible one to deform during the sintering stage at higher temperatures, while paste 3 richer in clayey materials is the most resistant one to pyroplastic deformation.

Fig. 3(f) show the evolution of apparent density of the tested compositions before and after being sintered at different temperatures. In comparison to the green density, the sintered density

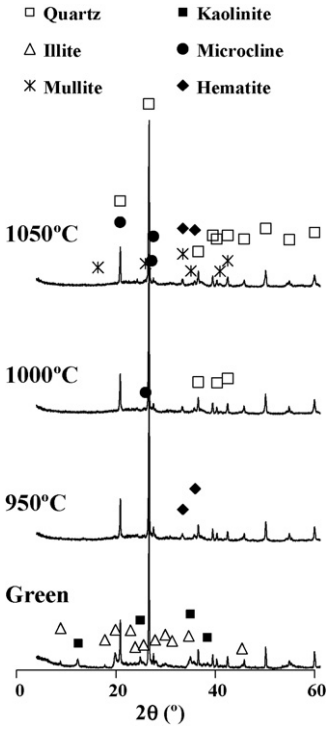

Fig. 4. XRD spectrogram for composition 2 before and after being sintered at several temperatures.

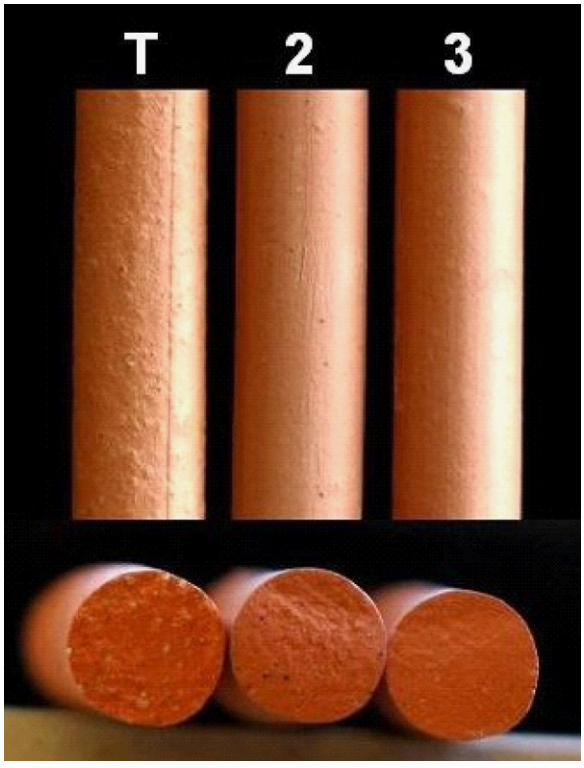

Fig. 5. Appearance of external surface and of the fracture cross-section of extruded cylinders sintered at 959 °C.

first decreases upon sintering at 950 °C due to the weight loss and the relatively low degree of densification, but tends to recover after firing at 1000 °C, overcoming the initial value with further densification at the highest temperature. This observation is in good agreement with the results shown in Fig. 3(b), allowing to conclude that the total porosity of the samples decreases with sintering temperature increasing.

Fig. 4 shows the XRD spectrogram for composition 2 before and after being sintered at different temperatures, as an example, since compositions 3 and T revealed similar spectograms, comprising the same crystalline phases: quartz, kaolinite, illite, microcline, mullite, and hematite. The mullite peaks could be clearly detected at 1050 °C especially for the compositions 2 and 3. The intensity of the quartz peaks tend to decrease with increasing sintering temperatures due to their gradual dissolution into glassy phase. This was more evident for composition 2. The intensity of fluxing minerals, illite included, tends to decrease for higher temperatures, as expected.

Formulation 2 (comprising 10 wt.% GS) showed the most promising results in terms of bending strength, followed closely by composition 3. The samples sintered at 959 °C in the industrial kiln presented water absorption values inferior to 6%, and superior bending strength before (∼14 MPa) and after firing (∼38 MPa) in comparison to commercial paste T, corresponding to increases of about 100 and 58%, respectively, as illustrated in Figs. 3(c). However, in terms of pyroplastic deformation index, composition 3 performs better than the other tested compositions due to its higher refractoriness conferred by its higher kaolinite content, being more closely followed by composition 2. The sintered samples of composition 2 showed rustic surface texture given by the iron particles present in the GS.

Fig. 5 shows the appearance of external and fracture cross-section surfaces of the extruded cylinders sintered at 959 °C. The close observation of the samples reveals that commercially composed T presents a rougher external surface due to the presence of coarser quartz grains in comparison to compositions 2 and 3. Some coarse quartz grains are also evidenced by the brighter spots at the fracture surface of T. Oppositely, composition 2 reveals small black points due to the iron particles introduced by the GS, while composition 3 exhibits a uniform coloured fracture. These observations are supported by the SEM microstructures and EDS elemental (Si, Fe) mapping of the fracture surfaces of the extruded cylinders sintered at 959 °C shown in Fig. 6. Large quartz grains are clearly seen in the reference paste, which came mostly from the low plasticity YC. The SEM microstructure of composition 2 (on the left side) exhibits a dark spot at the centre, which is iron rich as confirmed by the EDS

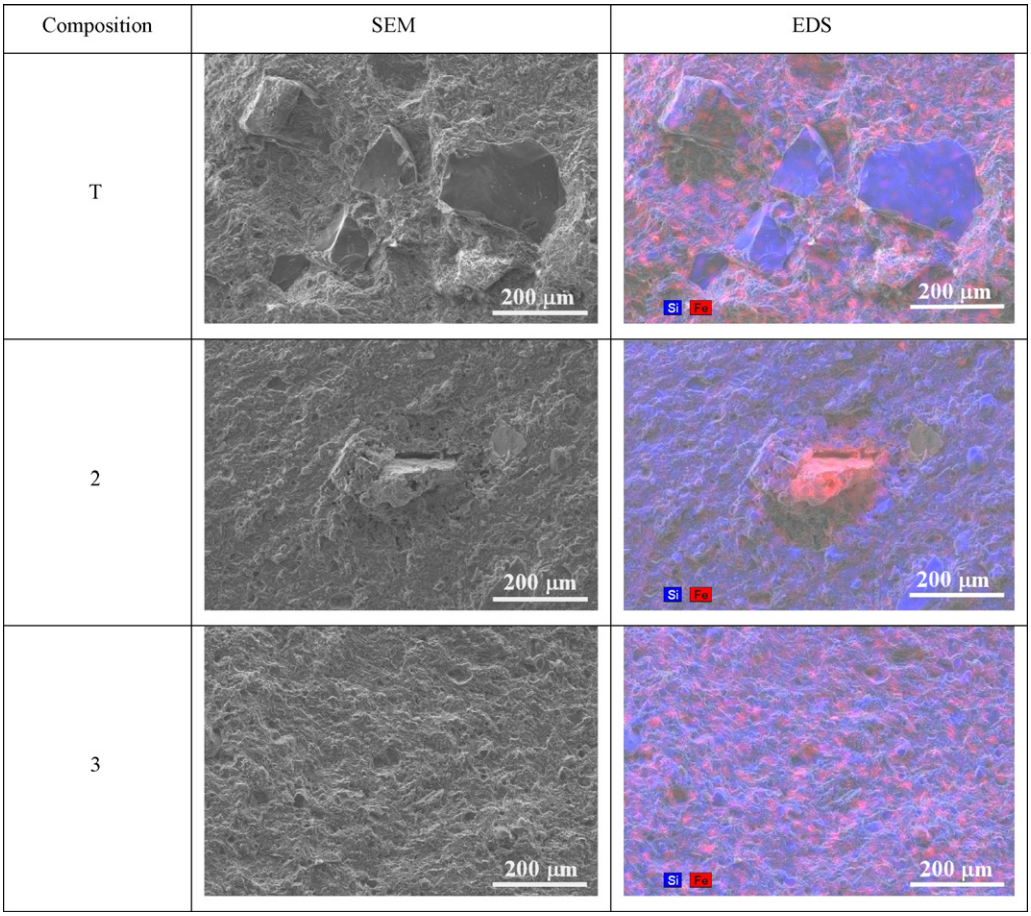

Fig. 6. Characteristic SEM microstructures and EDS elemental mapping of extruded cylinders sintered at 959 °C observed at the fracture surfaces after a three-point bending test. Si and Fe correspond to blue and red colours, respectively, in EDS elemental maps. (For interpretation of the references to colour in this figure legend, the reader is referred to the web version of the article.)

elemental mapping (on the right side). These results confirm the incorporation of iron particles in composition 2 by the granite sludge (10 wt.%, Table 1), being in good agreement with the high total iron content in GS, amounting to 10.63 wt.% when expressed as Fe_2O_3 (Table 2). The fracture surface of composition 3 shows the highest degree of homogeneity among all the samples, which is confirmed by the evenly distributed Si and Fe elements in EDS map. A similar degree of homogeneity has been also achieved in composition 2, being only disturbed by the localised black spot due to an iron-rich particle. The lower degree of microstructural uniformity observed in the reference paste, including the coarse quartz grains and the inevitable microcracks formed around them due to the mismatch of the coefficient of thermal expansion between the quartz grains and the red clay matrix, explain the higher water absorption values and the poorer mechanical properties of the sintered T samples in comparison to the new formulation incorporating industrial residues.

4. Conclusions

The results presented and discussed along this work enable to draw the following conclusions:

1. The inert granite sludge used is constituted by the same crystalline phases (quartz, albite, microcline, and illite) encountered in natural ceramic raw materials, enhancing the feasibility of its recycling in conventional ceramic formulations.
2. The high tonnage of raw materials consumed in the fabrication of bricks and roof tiles make their formulations suitable matrixes to incorporate this kind of residue replacing non-renewable natural resources.
3. The results presented in this work have shown that the need to reduce the burden of waste management, avoiding the negative impact associated with landfill and the danger it represents for the health, and of preserving natural resources by reusing industrial residues, should be regarded as a challenge and an opportunity to suitably reformulate the traditional ceramic compositions and keep or even improve the properties of the final products.
4. All of the above targets have been achieved in the present work. The products made of the new formulations incorporating industrial sludges are mechanically stronger, less porous (water absorption value <6%), and more resistant to pyroplastic deformation in comparison to the referred industrial products.

Acknowledgements

The financial support of CICECO is acknowledged. S.M. Olhero wishes to thank Foundation for Science and Technology (FCT) of Portugal for the financial support under the grant SFRH/BPD/27013/2006.

References

1. Directive 2006/21/EC of the European Parliament and of the Council of 15 March 2006 on the management of waste from extractive industries. *Off. J. L* 102/15, 11/04/2006 (http://eur-lex.europa.eu/).
2. Directive 2004/35/CE of the European Parliament and of the Council of 21 April 2004 on environmental liability with regard to the prevention and remedying of environmental damage. *Off. J. L* 143/56, 30/04/2004 (http://eur-lex.europa.eu/).
3. *Associação Brasileira da Indústria de Rochas Ornamentais—O sector das rochas ornamentais e de revestimento*, 2005 (in Portuguese).
4. INETI, PNAPRI, *Guia técnico do sector da pedra natural*, 2001 (in Portuguese).
5. Waste European List, Commission Decision 2000/532/EC of 3 May 2000, *Off. J. L* 226/3, 6/9/2000 (http://eur-lex.europa.eu/).
6. Velho, J., Gomes, C. and Romariz, C., *Minerais industriais: Geologia, Propriedades, Tratamentos, Aplicações, Especificações, Produções e Mercados*. Gráfica de Coimbra (Portugal), 1998, pp. 390–413 (in Portuguese).
7. Menezes, R. R., Ferreira, H. S., Neves, G. A. and Ferreira, H. C., Uso de rejeitos de granitos como matérias-primas cerâmicas. *Cerâmica*, 2002, **48**(306), 92–101.
8. Menezes, R. R., Estado de arte sobre o uso de resíduos como matérias-primas cerâmicas alternativas. *Revista Brasileira de Engenharia Agrícola e Ambiente*, 2002, **6**, 303–313.
9. Ferreira, J. M. F. and Mendonça, A. M., Inertization of galvanic sludges by its incorporation in ceramic products. *Boletin de la Sociedad Espanõla de Cerámica e Vidro*, 1999, **38**(2), 127–131.
10. Ferreira, J. M. F., Guedes, P. J. S. and Faim, P. F., Recycling of industrial residues: the best strategy for waste management, Al-Azhar Bulletin of Science. In *Proceedings of Fifth International Science Conference*, 2003, pp. 293–305.
11. Hernández-Crespo, M. S. and Rincón, J. Ma., New porcelainized stoneware materials obtained by recycling of MSW incinerator fly ashes and granite sawing residues. *Ceram. Int.*, 2001, **17**, 713–720.
12. Menezes, R. R., Ferreira, H. S., Neves, G. A., Lira, H. L. and Ferreira, H. C., Use of granite sawing wastes in the production of ceramic bricks and tiles. *J. Eur. Ceram. Soc.*, 2005, **25**, 1149–1158.
13. Vieira, C. M. F., Soares, T. M., Sánchez, R. and Monteiro, S. N., Incorporation of granite waste in red ceramics. *Mater. Sci. Eng. A*, 2004, **373**, 115–121.
14. Monteiro, N. S., Peçanha, L. A. and Vieira, C. M. F., Reformulation of roofing tiles body with addition of granite waste from sawing operations. *J. Eur. Ceram. Soc.*, 2004, **24**, 2349–2356.
15. Acchar, W., Vieira, F. A. and Hotza, D., Effect of marble and granite sludge in clay materials. *Mat. Sci. Eng. A*, 2006, **419**, 306–309.
16. Torres, P., Fernandes, H. R., Agathopoulos, S., Tulyaganov, D. and Ferreira, J. M. F., Incorporation of granite cutting sludge in industrial porcelain tile formulations. *J. Eur. Ceram. Soc.*, 2004, **24**, 3177–3185.
17. Torres, P., Manjate, R. S., Quaresma, S., Fernandes, H. R. and Ferreira, J. M. F., Development of ceramic floor tile compositions based on quartzite and quartzite sludges. *J. Eur. Ceram. Soc.*, 2007, **27**, 4649–4655.
18. International Organization for Standardization, ISO 10545-3, *Ceramic Tiles—Part 3*. International Organization for Standardization, 1995.
19. Sigg, J., *Les Produit de Terre Cuite: Matérias Premières, Fabrication, Caractéristiques, Aplications—Faiences et Grés*. Editions Septima, Paris, 1991.
20. Grim, R. E., *Applied Clay Mineralogy*. McGraw-Hill, New York, 1962.
21. Gippini, E., *Pastas cerâmicas*. Sociedade Espanhola de Cerâmica, Madrid, 1979.
22. Jouenne, C. A., *Traité de Céramiques et Matériaux Minéraux*. Editions Septima, Paris, 1979.
23. McConville, C. J. and Lee, W. E., Microstructural development on firing illite and smectite clays compared with that in kaolinite. *J. Am. Ceram. Soc.*, 2005, **88**(8), 2267–2276.
24. Iqbal, Y. and Lee, W. E., Fired porcelain microstructure revisited. *J. Am. Ceram. Soc.*, 1999, **82**(12), 3584–3590.